Modeling the Influence of the Composition of Refractory Elements on the Heat Resistance of Nickel Alloys by a Deep Learning Artificial Neural Network

Dmitry A. Tarasov[1,a)], Oleg B. Milder[1,b)], Andrey G. Tyagunov[1,c)]

[1]*Ural Federal University, Mira str., 19, Ekaterinburg, RUSSIA 620002*

[a)]Corresponding author: datarasov@yandex.ru
[b)]milder@mail.ru
[c)]adi8@yandex.ru

Abstract. Nickel alloys are widely used in the production of gas turbine parts. The alloys show resistance to mechanical and chemical degradation under severe long-term stress and high temperatures. One of the major mechanical properties of the alloys is the high-temperature rupture strength, which is measured after a specimen is heated to a certain temperature and held for a certain time considering deformation. Determining the influence of certain elements on the properties of an alloy is a complex scientific and engineering problem that affects the time and cost of developing new materials. Simulation is a great chance to cut costs. In this paper, we predict a high-temperature strength based on the composition of refractory elements in alloys using a deep learning artificial neural network. We build the model based on prior knowledge of the composition of the alloys, information on the role of alloying elements, type of crystallization, test temperature and time, and the tensile strength. Successful simulation results show the applicability of this method in practice.

Keywords: Nickel alloys; Rupture strength; Heat resistance; Deep learning; Modeling.

1. INTRODUCTION

Nickel alloys are commonly used for gas turbine engine parts and other heat-resistant device manufacturing, which makes them extremely important for the industry. The turbine parts operate in an extremely aggressive and highly corrosive environment under high pressures. Thus, the high-temperature materials should possess adequate resistance to creep, fatigue, and other negative phenomena. The situation is also complicated by the current growth of the turbine entry temperature, which provides a greater engine thrust and better fuel efficiency.

The development of materials with such unique properties is a challenging engineering task requiring a concentration of modeling and experimental efforts. Continuous improvement of alloy characteristics is achieved not only through the use of diverse, often quite exotic, alloying, but also with the help of specialized protective coatings, as well as, through directional solidification (DS) of either columnar grains or single crystals (SX) along with the most favorable crystallographic texture [1].

The hardening mechanisms of nickel alloys have been studied in detail. It was experimentally proven that the main contribution to the hardening is made by γ' and γ'' precipitates. Other phases of intermetallic precipitation, such as carbides and nitrides, significantly less affect the mechanical properties, however, they contribute to creep and rupture due to their influence on the behavior of grain boundaries under loads. During casting, fine particles dispersed in a nickel matrix form a wavy frame and act as a barrier to the movement of the dislocations, which leads to an increase in hardening. The behavior of precipitates in alloys is dependent on temperature.

The spatial characteristics of the alloys also have an ambiguous effect. Typically, the precipitates and matrix have a slight misorientation of the lattice. However, with increasing temperature, there is a tendency to intersect the

dislocation in the γ precipitate phase with the {100} plane, which may lead to an increase in γ' hardening [2]. To achieve the strongest hardening effect of a solid solution, it is important to choose alloying elements that can provide the greatest magnitude of lattice deformation without causing the formation of new phase components [3].

The recent advances in single-crystal alloy strengthening have been accomplished by the incorporation of "heavy" refractory elements, such as molybdenum, tungsten, niobium, tantalum, rhenium, and ruthenium into the alloys. This inhibits the atomic diffusion process, however, it may also lead to the precipitation of undesirable phases, unpredictable behavior of the alloying mixture, and, besides, lead to a significant increase in production costs. It is the growth in the cost of alloy components that, on the one hand, complicates the conduct of large-scale experiments, and, on the other hand, prevents the widespread use of new alloys.

The major mechanical properties of the alloys are tensile yield stress, ultimate tensile strength, rupture life, creep, fatigue, *etc.* However, in different countries (and even in various scientific communities), not only the names of the properties differ, but also the test methods determining these properties do. All this significantly complicates the analysis and the mutual correlation of experimental results.

The set of properties that most accurately reflects the extreme characteristics of the alloy under operating conditions inside a gas turbine (long exposures at high temperature and pressure) up to the failure of the part is the high-temperature creep and the rupture strength.

Temperature growth leads to an increase in the thermal motion of alloy atoms, which, in turn, is the cause of greater mobility of dislocations, increase amount of vacancies, deformation at grain boundaries, and metallurgical changes, *i.e.,* phase transformation, precipitation, oxidation, and recrystallization. Creep (or a time-dependent increase in the length of an alloy specimen) occurs when a metal is subjected to a constant tensile load at an elevated temperature.

According to ASTM E139-11(2018) [4], the creep test is carried out by applying a constant load to a tensile specimen maintained at a constant temperature. In the creep tests, the creep curves (Fig.1) are obtained [5, Unit 1]. Typical creep curve showing three distinct stages with different creep rates. After an initial rapid elongation, the creep rate decrease with time until reaching the steady-state (secondary creep), and then (tertiary creep) yields a rapid creep rate until failure. Primary creep is a period of transient creep; the creep resistance of the material increases due to material deformation. Secondary creep provides a nearly constant creep rate; the average value of the creep rate during this period is called the minimum creep rate. Tertiary creep shows a rapid increase in the creep rate due to the effectively reduced cross-sectional area of the specimen.

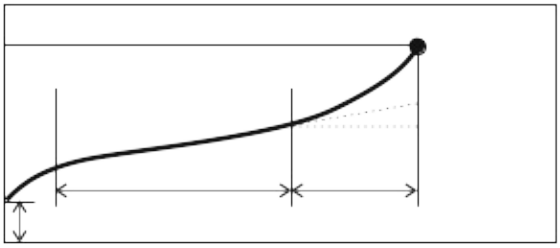

FIGURE 1. A typical creep curve

While the creep tests measure the dimensional changes that occur when a specimen is subjected to high temperature, the rupture tests measure the effect of temperature on the longtime load-bearing characteristics. The rupture tests are carried out similarly to the creep ones, however, they go at a higher strain level (and usually smaller times), until the specimen fails and the time to failure (*i.e.* rupture life) is measured. Stress-rupture curves usually show a straight line (Fig. 2) [5, Unit 5]. Changing the slope indicates structural changes in the material, *i.e.*, transgranular or intergranular fracture, oxidation, recrystallization, grain growth, spheroidization, and precipitation.

On the other hand, the Russian standard ГОСТ 3248-81 [6] offers a slightly different method of creep measurement. According to the standard, the specimen should be installed in the grips of the testing machine and placed in the furnace where it is heated to a predetermined temperature (heating time should be no more than 8 hours) and kept at this temperature for at least 1 hour. If necessary, the exposure time is regulated in the standards or technical conditions for metal products. After heating and holding at a given temperature, a preload of approximately 10% of the given total load is smoothly applied to the specimen, however, the preload should not

cause a strain of more than 10 MPa. If the temperature of the specimen and the readings of the elongation meter remain unchanged for 5 minutes, then the specimen is gently loaded to a predetermined strain. Simultaneously with the load, the elongation of the specimen should be recorded, starting with the preliminary load and at each loading stage, if the latter is carried out in stages. The records of the rupture test results, hence, contain rupture strength correspond to the given temperature and given time. Besides, the times and temperatures are selected from the pre-set suite: times in hours are usually 100, 500, 1000, 5000, *etc.*; temperatures in °C are usually 800, 850, 900, *etc.* up to 1200.

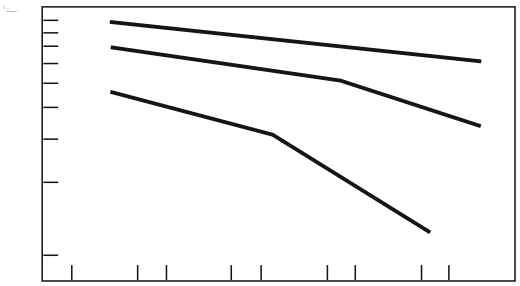

FIGURE 2. Typical stress-rupture curves (in log-log scale).

Despite the differences in approach, the Western and Russian creep and rupture test results might be brought easily. As it has been shown [7, p.312], time (τ), temperature (T), and stress (σ) are independent variables combined in the creep behavior function ε (1). In other words, we can expect similar creep or rupture indicators achieved by two different experimental strategies. All available alloys are compared with each other, regardless of the test method.

$$\varepsilon = f_1(\sigma) f_2(\tau) f_3(T), \qquad ()$$

Alloys design and analysis require a large number of experiments to carry out. Since physical modeling is time-consuming and quite expensive, in particular, taking into account the ever-increasing cost of refractory elements that make up alloys such as W, Mo, Nb, Ta, Re, Ru. The mathematical simulation could be a promising alternative. Novel simulation techniques like artificial neural networks (ANNs) make it possible to extrapolate the known results of tests for the long-term strengths without the implementation of the full-scale experiments. The use of neural networks is suitable for modeling correlations that are blurry, difficult to describe, or cannot be accurately simulated by the physical models [8]. This is the major reason for applying neural modeling in such a complicated task like alloys properties simulation. The key problem in modeling is the fact that the alloys are usually tested in fairly narrow time and temperature ranges that leads to the insufficient volume of an initial database for building the models. Moreover, it is extremely difficult to solve the problem of taking into account the influence of one or another element, or a group of elements. In particular, this applies to expensive refractory elements.

Previously, the ANNs were used to analyze the nickel alloys, however, the major goal of these works was to synthesize new chemical compositions of the alloys [9–14]. There are, also, the ANN applications to model change in the coefficient of thermal expansion [15, 16], to model energy hysteresis [17], to predict low-cycle fatigue energy [18], to model the development of fatigue cracks [19], to predict the occurrence of material defects [20], and to model the time to failure [21]. We also engaged ANN approach to replenish the missing nickel alloys properties [22].

This work aims to establish relationships between the refractory elements content and the rupture strength in the nickel alloys by means of the deep learning artificial neural network.

2. APPROACH AND EXPERIMENTAL

To carry out the experiment, we have collected the database on Russian and Western nickel alloys, their chemical

compositions and mechanical properties, which contains information on about 350 nickel alloys with known content and properties. All the data forms about 2700 individual samples acting as the model inputs. Usually, alloys from the sample have information on averagely five results of testing (time τ, temperature t, and rupture strength σ). All samples have at least some of the refractory elements W, Mo, Nb, Ta, Re, Ru in the content. This sample acts as a training set for the artificial neural network.

As an independent verification sample to evaluate the model results, we use the alloys data (time to rupture for several temperature and stress conditions) corresponding to expression (3) from the US patents [23–25]. The data from the verification sample in no way participated in the processes of neural networks training.

Since the rupture strength range in experiments covers a band of several orders of magnitude, we use its logarithmic transformation $y = lg\,\sigma$ that, also, makes prediction errors relative. Moreover, the model target values (y) for the inverse transformation $\sigma = 10^{y}$ exclude the possibility of negative σ values, which are physically impossible. All this improves the performance of the model.

The previous attempts to model the alloys features by mean of artificial neural networks [26] have shown that the Bayesian regularized artificial neural network (BRANN) are more robust than standard back-propagation ones, are able to reduce or even eliminate the need of cross-validation, and have shown satisfactory predictive ability along with resistance to overtraining. However, in this experiment, even the BRANN might not be enough to gain the desired performance, since we need to append more complicated additional information into the model.

Together with the information on the chemical content in the alloy, in order to increase the accuracy of forecasting, we added the data on the type of solidification (equiaxed, directional, or single-crystal). These data, the test time (τ), and absolute temperature (T=273+t) form a "casting vector" (CV) that feed to the separate model input. Moreover, we, also, take into account the role of alloying elements in alloys strengthening. According to [27, p.29], some doping strengthen the nickel matrix by creating a solid solution, other forms excess phases: intermetallides, carbides, borides *etc.* These roles are combined in Table 1.

TABLE 1. ROLES OF ALLOYING ELEMENTS IN ALLOYS PROPERTIES

No	Effect	Alloying elements
1	Solid solution strengtheners	Co, Cr, Fe, Mo, W, Ta, Re
2	Carbide form MC	W, Ta, Ti, Mo, Nb, Hf
3	Carbide form M_7C_3	Cr
4	Carbide form $M_{23}C_6$	Cr, Mo, W
5	Carbide form M_6C	Mo, W, Nb
6	Carbonitrides: M(CN)	C, N
7	Forms γ' Ni_3(Al, Ti)	Al, Ti
8	Raises solvus temperature of γ'	Co
9	Hardening precipitates and/or Intermetallides	Al, Ti, Nb
10	Oxidation resistance	Al, Cr, Y, La, Ce
11	Improve hot corrosion resistance	La, Th
12	Sulfidation resistance	Cr, Co, Si
13	Improves creep properties	B, Ta
14	Increases rupture strength	B
15	Grain-boundary refiners	B, C, Zr, Hf
16	Retard coarsening	Re, Ru

Previously, the role of alloying elements was considered individually, which generated a lot of conflicting information in the models. Now, we combine he roles in the interconnection matrix (Table 2) that reflects how each chemical element or the casting vector affects the alloys mechanical property. It should be noted that different refractory elements contribute to different mechanisms that appear in the alloys.

To be able to account such complication, we engage a deep learning artificial neural network (DLANN) where the interconnection matrix plays the role of a trigger that passes or does not pass a corresponding signal to the next layer. The DLANN framework built in Matlab. The network is a non-fully connected perceptron, in which separate

groups of neurons of the first hidden layer are responsible to count the specific role of the alloying elements in accordance with the interconnection matrix.

As reference data on the effect of refractory elements on the properties of nickel alloys, we used the results of the work of [28]. We also provide an illustration from the work (Fig. 3). The work displays the rupture test results of 1000 ºC and 100 hours (σ_{100}^{1000}) depending on the total content of refractory elements for a number of nickel alloys. In addition, the distribution of these alloys by generations is illustrated. Fig. 3 clearly shows that with an increase in the generation number of the alloy, both its mechanical properties and the total composition of refractory elements, and hence the price, increase.

TABLE 2. THE INTERCONNECTION MATRIX; "1" MEANS PRESENCE OF LINKAGE

Element/ Role	SSH[2]	MC[3]	M_7C_3	$M_{23}C_6$	M_6C	γ'	OxRes[4]	S_Res[5]	Im_Crp[6]	Gr_Bnd[7]	GPR[8]	Tsld_Up[9]	Rest[10]	Out[11]
C		1	1	1	1					1				1
Cr	1		1	1			1	1						
Co	1							1						1
Mo	1	1		1	1									
W	1	1		1	1							1		
Al						1	1							
Ti		1				1		1						
Nb		1			1	1								
B									1	1				1
Fe	1													
Zr										1				
Ta	1	1				1			1					
Re	1										1	1		
Ru	1										1			
V		1												
Ce							1							
La							1							
S													1	
Si								1						
Mn													1	
P													1	
Hf		1				1				1				
CV[1]	1	1	1	1	1	1	1	1	1	1	1	1	1	1

[1] CV is the Casting Vector combining the solidification type, crystallographic direction of crystallization, test time (τ), and test temperature (T); [2] SSH is the solid solution hardening; [3] M_xC_y are carbides; [4] is the oxidation resistance; [5] is the sulfidation resistance; [6] improves creep properties; [7] are grain-boundary refiners; [8] retard γ' coarsening; [9] increases solidus temperature; [10] rest impurities; [11] connections to the output layer

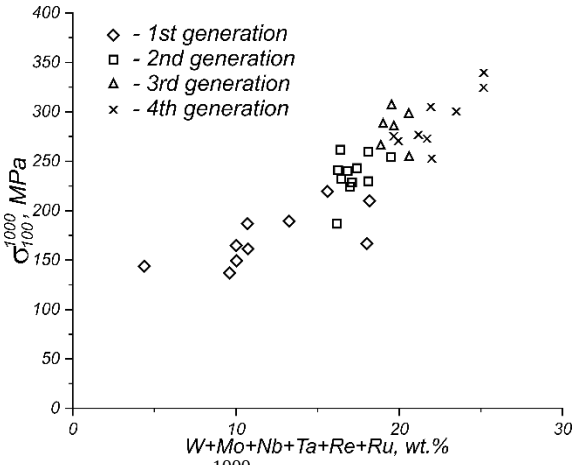

FIGURE 3. The dependence of the rupture strength (σ_{100}^{1000}) on the total amount of the refractory elements in the nickel alloys; the generations of the alloys are also depicted.

Thus, we train the network by the full database (training set) and then predict the σ_{100}^{1000} for the nickel alloys sub-sample (about 170 alloys that contain all the refractory elements) and compare the results with that from [28]. In order to evaluate the prediction accuracy, we use the absolute value of the relative error (RE) between the DLANN predictions and the real data from the verification sample.

$$\Re_i = ¿¿ \quad (1)$$

3. RESULTS AND DISCUSSION

We must emphasize that the trained DLANN predicted the results of only one rupture test condition: 1000 ºC and 100 hours (σ_{100}^{1000}) for different alloy compositions. With this approach, it is convenient to represent predictions graphically (see Fig. 4). The result is in good agreement with the results [28]. If we compare Fig. 3 and Fig. 4, we may deduce that the model's predictions are consistent with the experimentally observed results. This confirms the adequacy of the model and is its indirect validation. One extremely difference between these results is that the first required a lot of effort of a large group of researchers, a long time, and significant material costs, while the second one required only a few minutes of calculations on the most ordinary home laptop.

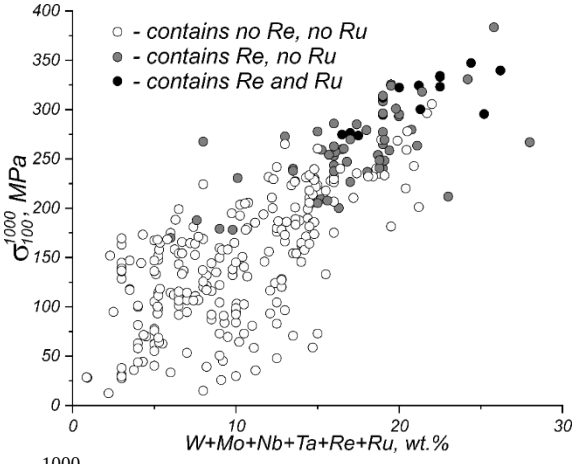

FIGURE 4. Results of the model σ_{100}^{1000} predictions depending on the total amount of the refractory elements; the content of rhenium and ruthenium is also indicated by the shade.

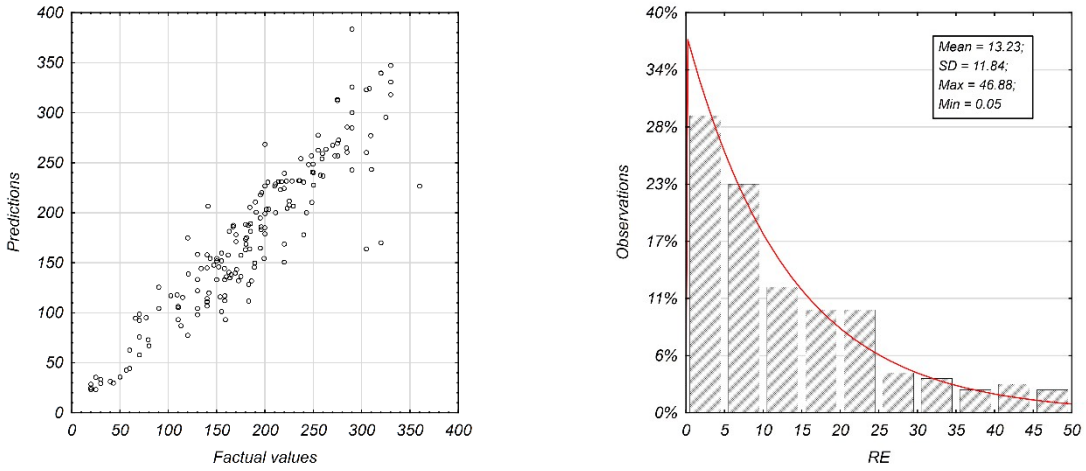

(a) (b)

FIGURE 5. Results of the model precision evaluation: (a) spread and (b) relative error (%) distribution with the exponential fit.

The model precision evaluation has been carried out using the method of predictions of the "unknown" for the model values from the verification data set. The spread between the predictions and the real values is shown in Fig. 5(a). The distribution of the relative error (RE) between predictions and the real data we may see in Fig. 5(b). Analyzing the depicted information, we may consider the model performance satisfactory. The 75% quantile of the relative error distribution does not exceed 20%. This is similar to the accuracy of the results of full-scale physical experiments. By increasing the training sample and refining the aspects of the influence of elements on the properties of the alloys, we will increase the accuracy of modeling.

4. CONCLUSION

The main problem with the use of refractory elements in the composition of heat-resistant nickel alloys is their cost. The development and analysis of alloy properties is an extremely laborious and time-consuming procedure, and the cost of the work of huge teams is added to the cost of the elements themselves. Simulation using artificial neural networks has shown its advantages, such as speed and accuracy. This work was devoted to the application of this technique to assess the effect of the content of refractory elements on the heat resistance of nickel alloys.

Taking a trained neural network as a basis, we simulated the results of a real experiment described in 28. Our model showed its best side. An independent assessment of the forecast accuracy showed an error not exceeding 20%. Taking into account the negligible cost of a computational experiment in comparison with a full-scale experiment, we can conclude that the proposed technique is extremely promising.

REFERENCES

[1] N. Das, *Trans Indian Inst Met*, **63**(2–3), 265–274 (2010).
[2] Y. Zhou, Z. Zhang, Z. Zhao et al. *Rare Metals* **31**(3), 221–226 (2012).
[3] M. Detrois, J. Rotella, M. Hardy et al. *Integr Mater Manuf Innov* **6**(4), 265–278 (2017).
[4] ASTM E139-11(2018) Standard Test Methods for Conducting Creep, Creep-Rupture, and Stress-Rupture Tests of Metallic Materials.
[5] H. E. Boyer, *Atlas of Creep and Stress-Rupture Curves* (ASM int., 1988).
[6] ГОСТ 3248-81 Металлы. Метод испытания на ползучесть. (Metals. The creep test method) (in Russian).
[7] J. Pelleg, *Mechanical Properties of Materials* (Springer, 2013).
[8] S. O. Haykin, *Neural Networks and Learning Machines* (3rd ed,, McMaster University, Ontario Canada, 2009).
[9] Y. S. Yoo, I. S. Kim, D. H. Kim, C. Y. Jo, H. M. Kim, C. N. Jone, "The application of neural network to the development of single crystal superalloys, in *Superalloys* (Ed. by K.A. Green, TMS, 2004).
[10] O. S. Nurgayanova and A. A. Ganeev, *Polzunovsky almanac* **3**, 22–26 (2006) (in Russian).

[11] O. S. Nurgayanova and A. A. Ganeev, *Neurocomputers: development, application* **10**, 70–74 (2007) (in Russian).
[12] O. S. Nurgayanova and A. A. Ganeev, *Bulletin of Ufa State Aviation Technical University*, **9**(1), 160–169 2007 (in Russian).
[13] O. S. Nurgayanova and A. A. Ganeev, *Bulletin of Ufa State Aviation Technical University*, **8**(4), 91–95 (2006) (in Russian).
[14] O. S. Nurgayanova and A. A. Ganeev, *Polzunovsky almanac* **3**, 22–26 (2006) (in Russian).
[15] N. Bano, A. Fahim, and M. Nganbe "Determination of Thermal Expansion Coefficient of IN738LC with Duplex Size Gamma Prime using Neural Network" in *Proceedings of the Conference of Metallurgists* (Winnipeg, 2008).
[16] N. Bano and M. Nganbe, *J.Mat.Eng.Perform*. **22**(4), 952–957 (2013).
[17] N. Bano and M. Nganbe "Neural Network Approach for Modeling the Hysteresis Energy of Ni based Superalloys" in *Proceedings of the International Conference on Mechanical Engineering and Mechatronics*, (Ottawa, 2012).
[18] N. Bano, A. Fahim, and M. Nganbe "Neural Network Model to Predict Low Cycle Fatigue Failure Energy of Rene77" in *Proceedings of the AES-ATEMA'2010 Fifth International Conference*, (Montreal, Quebec, Canada, 2010), pp. 123–126.
[19] N. Bano, A. Fahim, and M. Nganbe "Fatigue Crack Initiation Life Prediction of IN738LC using Artificial Neural Network" in *Proceedings of the AES-ATEMA'2010 Fifth International Conference*, (Montreal, Quebec, Canada, 2010), pp. 117–121.
[20] S. Feng, H. Zhou, H. Dong, *Mat.&Design* **162**, 300–310 (2019).
[21] M.H. Hasan, M. Al Hazza, W. Mubarak, *J.Automat.Control Eng,* **2**(4), 353–356 (2014).
[22] A. Tyagunov, O. Milder, D. Tarasov, "Application of Artificial Neural Networks for the Replenishment of Nickel-based Superalloys Catalogues" in *Proceedings 2nd European Conference on Electrical Engineering & Computer Science EECS 2018* (IEEE Explore, 2019), pp. 41–44.
[23] US patent 2004/0177901 A1.
[24] US patent 6,673,308 B2.
[25] US patent 6,051,083.
[26] A. Tyagunov, O. Milder, D. Tarasov, *WSEAS Trans Env. Dvlp*, **15**, 113–119 (2019).
[27] M. J. Donachie, S. J. Donachie, *Superalloys: A Technical Guide* (2nd Ed., ASM Int., 2002).
[28] A.V. Logunov, I.A. Leshchenko, D.V. Danilov, I.I. Khryaschev, S.A. Zavodov, I.V. Ilyin, "Development of a rhenium-free high-heat-resistant nickel alloy for monocrystalline turbine blades, mastering its production and manufacturing of parts from it" (in Russian). Available online: http://www.aviationunion.ru/Files/Nom_4_SATURN.pdf (accessed on 10 June 2020).